CHAPTER 136

IMPACT BREAKING WAVE PRESSURES ON VERTICAL WALLS

Masataro HATTORI[1] and Atsusi ARAMI[2]

ABSTRACT

Impact wave pressures acting on a vertical wall were dis-
cussed by simultaneous measurements of the pressure and wave shapes
at impact.
Experiments confirmed the principal role of adiabatic proc-
esses of trapped air bubbles to the generation of impact pressures.
The most severe impulsive pressure was observed when breaking waves
hit the wall with trapping small air bubbles or a very thin lens-
shaped air pocket. The larger the amount of the entrapped air, the
lower the magnitude of the impact pressures. Due to the pulsation
of the air pocket, damped pressure oscillations were observed
immediately after the impact pressure.
A predictive model, taking account of the adiabatic compres-
sion processes of the trapped air pocket, predicts fairly well the
maximum impact pressure and the frequency of the damped pressure
oscillation, in the case when plunging breakers collide against the
wall.

1. INTRODUCTION

Impact pressures have been considered unlikely to be effec-
tive for sliding and overturning massive structures seawalls.
Nevertheless, some studies (Weggel and Maxwell, 1970; Mogridge and
Jamieson, 1980; Arami and Hattori, 1988) and recent field observa-
tions pointed out a clear evidence that such pressures can cause
severe local damages to vertical wall type structures, and that the
resulting damages would develop owing to successive attacks of
breaking waves and cause sudden failures of the structures.
Since Bagnold (1939) proposed an air pocket model for the
physics of the high impulsive wave pressure, many experimental
studies have been performed to explicate the physics of wave-

---

1) Department of Civil Engineering, Chuo University, Tokyo
2) Ishikawajima-Harima Heavy Industries Co., Ltd., Tokyo

impact processes. However, published data from the various studies
provide very wide and different views on the wave-impact physics.
Therefore, more detailed and reliable examinations on this process
are absolutely necessary to the development of physical models
predicting for the impact pressure. The principal aims of this
study are as follows;
1. To explicate the difference of the wave-impact processes under
    various colliding conditions of breaking waves onto the wall,
2. To examine aerodynamic contributions of the entrapped air to the
    generation of the impact pressure, and
3. To propose a predictive model, taking account of adiabatic
    compression processes of the air pocket entrapped between the
    structure and wave.

2. EXPERIMENTAL EQUIPMENT AND PROCEDURES

2.1 EXPERIMENTAL EQUIPMENT

        General arrangement of the experimental equipment is shown in
Fig. 1. Experiments were carried out in a glass-walled wave flume,
0.30 m wide, 0.55 m high, and 20 m long, in which a steel beach of
1/20 slope was installed. Regular waves were produced by a reflec-
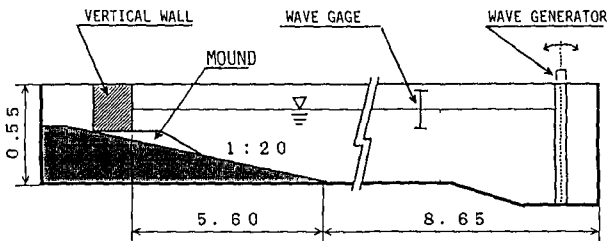tion-absorbing wave maker of flat type.

Fig. 1 General arrangement of the experimental equipment. (Units:m)

        Vertical plane wall of a 35 mm thick plastic plate (0.30 m
wide and 0.50 m high) was shored up with steel frames. The wall
complex, having a natural frequency of 1.2 KHz in water, was mount-
ed rigidly on a plastic mound with a foreshore slope of 1/10. Inci-
dent wave properties were detected by a capacitance-type wave gauge
installed at the uniform water depth.

2.2 PRESSURE MEASUREMENTS

        Impact pressures were measured by semi-conductor type trans-
ducers of 10mm in diameter. The pressure transducers have opera-
tional capacity of 100 gf/cm^2 and 200 gf/cm^2, with 100% overload
capability. Their natural frequency in water is 9.6 KHz and the
frequency response range DC to 4.8 KHz.
        Four pressure transducers were located vertically along the
centerline of the wall at an interval of 2.0 cm. The maximum impact
pressure is occurred most likely in the vicinity of the still

water level. Hence, two additional pressure transducers were set at
1.0 cm below and above the still water level and 5.0 cm apart from
the centerline.

2.3 RECORDING THE IMPINGING BREAKING WAVE PROFILE

High-speed videos were simultaneously taken at 200 frames/s
with the measurements of impact pressures. Photo. 1 is an example
of the picture of wave shape at impact. Number of the last three
digits on the top of the picture indicates the elapsed time in
millisecond after the start of a test run. White arrows on the left
hand side show the locations of the pressure transducers. Real-time
pressure record from the pressure transducer (P_4) at the still
water level is monitored on the left hand side of the still. The
synchronization between the pressure records and sequential stills
was made by using the pressure monitor within an accuracy of 0.1ms.

Length measurements were made using a 1.0 cm square grid
system, attached on the sidewall glass. The breaking wave height,
the size and shape of trapped air pocket, the forward and upward
velocities of wave surface at and in front of the wall were read
from the pictures projected on a 29-inch video-screen.

2.4 EXPERIMENTAL PROCEDURES

In the repeated tests,
impact pressures vary signifi-
cantly owing to the instabili-
ty of the wave breaking and
the high reflection of the
wall. We employed the two
following procedures to ensure
the repeatability of the
experiments; (1) Every test
run was made after the free
surface disturbance due to the
preceding test run was well
subsided, and (2) The wave
generator was controlled by a
programmed analogue signal
yielding a regular wave train.

Photo. 1 Example of
the video picture.

Outputs of the impact pressures were recorded on digital
recorders over six wave periods at a sampling frequency of 5 KHz
for extensive processing by computer. Data analyses were made for
four subsequent breaking waves preceded by some non-breaking waves.

3. EXPERIMENTAL RESULTS OF THE IMPACT PRESSURE CHARACTERISTICS

Since wave-impact processes depend closely on the wall loca-
tion relative to the wave breaking position (Chen and Melville,
1988), it is reasonable to characterize them by the development of
wave breaking at the wall, or the colliding conditions. In this
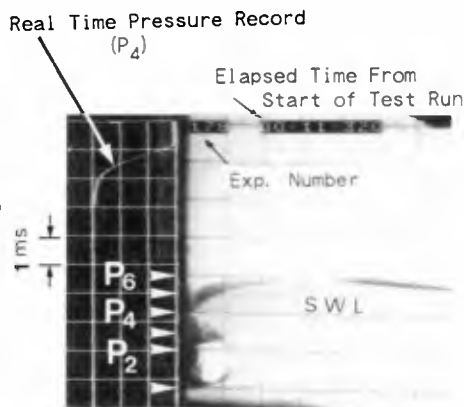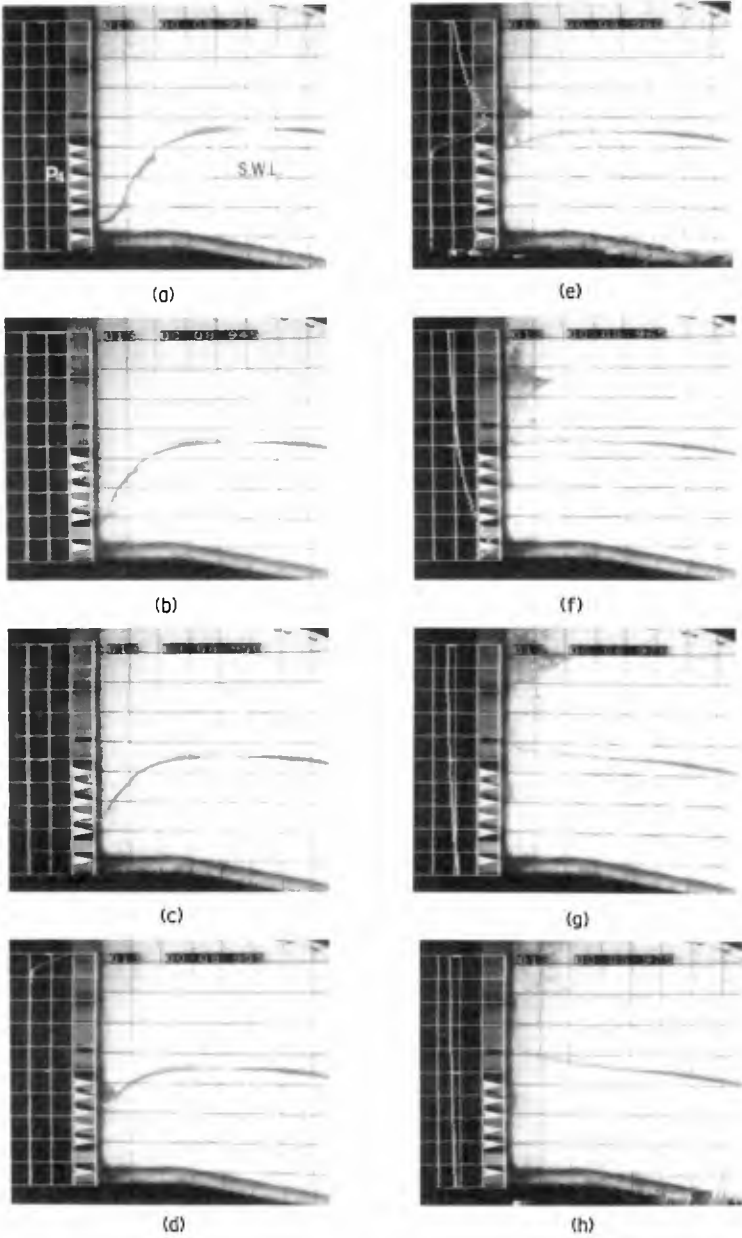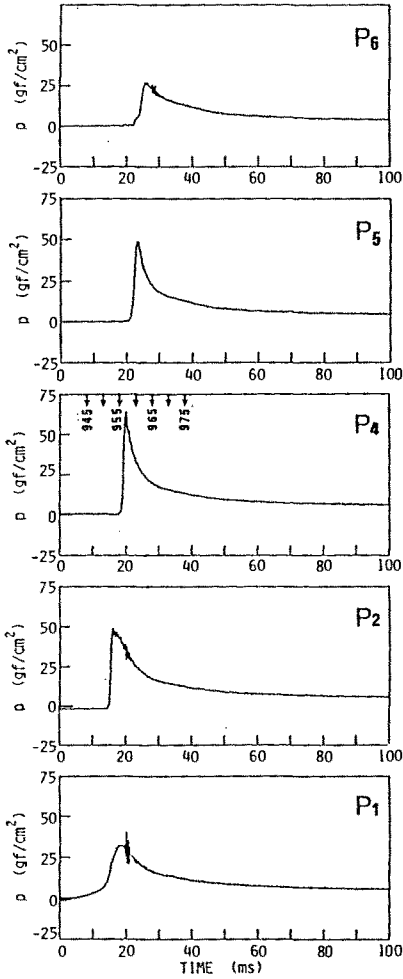study, we will examine into the essential characteristics of

Photo. 2   Sequence of the still pictures of the wave surface.
(Flip-through condition)

WAVE PRESSURE RECORDS (No. 013-3)
    FOR THE FLIP-THROUGH IMPACT.
H_i = 4.7 cm,   T = 1.7 s
H_b = 5.7 cm, i = 0
h_d = 2.5 cm.
P_{max} / $\rho g H_b$ = 11.2

Fig. 2 Wave pressure records (Flip-through condition)
        (H_b=5.7cm, T=1.7s)

impact pressures for the four following conditions, somewhat
similar to Oumeraci, Klammer, and Partenscky (1991);
(1) " Flip-Through" condition with no air bubbles,
(2) Collision of the vertically flat wave front with entrapping
    small air bubbles -- single peak pressure --,
(3) Collision of plunging breakers with a thin air pocket
    -- damped pressure oscillations with high frequencies --, and
(4) Collision of fully developed plunging breakers with a thick air
    pocket-- damped pressure oscillation with low frequencies --.

3.1 FLIP-THROUGH COLLISION WITH NO AIR BUBBLES.

Impact process due to the " flip-through" action (Cooker and
Peregrine, 1991) is observed when incident waves break as upward
deflected breaker near the wall. Photo 2, consisting of 8 still
pictures, gives the wave shape changes during the collision on the
wall. We notice from the sequential pictures that the wave shapes
change a very similar process to the computation by Cooker and
Peregrine(1991). The corresponding pressure records at various
elevations are given in Fig. 2, in which 20 ms on the time axis
refers to the time of the maximum peak pressure recorded at P_4, on
the still water level. Thick arrows on the top of the pressure
record at P_4 represent the shooting instant of the pictures.
Although the resultant peak pressures are not so high in the
magnitude $(p_{max, 4}/\rho gH_b = 11.2)$, the pressure record at P_4 shows that
an impact is occurred without a clear hit of the wave front.

3.2 COLLISION OF VERTICALLY FLAT WAVE FRONT WITH SMALL AIR BUBBLES
      -- SINGLE PEAK IMPACT PRESSURE --.

Collision of breaking waves with vertical or slightly curled
front brings about extremely high impact pressures $(p_{max,}/$
$\rho gH_b = 109.6)$, as seen in Photo. 3 and Fig. 3. However, even the
highest impact at P_4 is much lower than that due to a water hammer
process.
The pictures about the instant of collision (Photo. 3 (e) and
(f)) do not show apparently the air entrainment. But we can find
out dark image indicating a group of small air bubbles trapped over
the hitting region of wave crest (Photo. 3 (g) and (f)). The pres-
sure records in this region (Fig. 3 $P_1 - P_3$) exhibit clear pressure
fluctuations with very high frequencies of about 1,000 Hz during
the impact. The peak pressures occur simultaneously at various
elevations, but their magnitudes decrease remarkably with the
distance from the hitting point of the wave crest.
If a small air pocket in a form of very thin lens is trapped
in the vicinity of the impinging region of the wave crest, the
pocket is collapsed into small air bubbles at impact. This also re-
sults in a single peak impact pressure. Occasionally we observed a
fact that a fraction of the air bubbles was released upwards with
wave splash. This results in noticeable reduction of the peak
pressure and causes variability in the pressure magnitude. The
experiments, however, confirm an important role of the trapped air
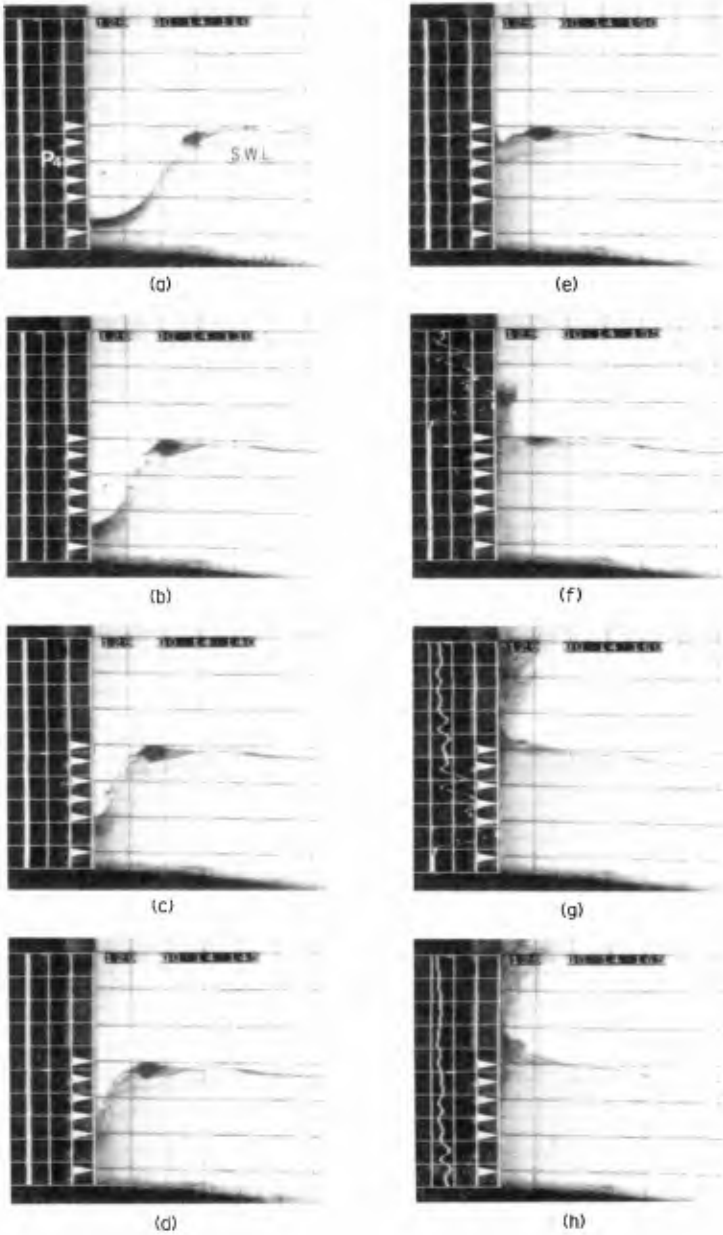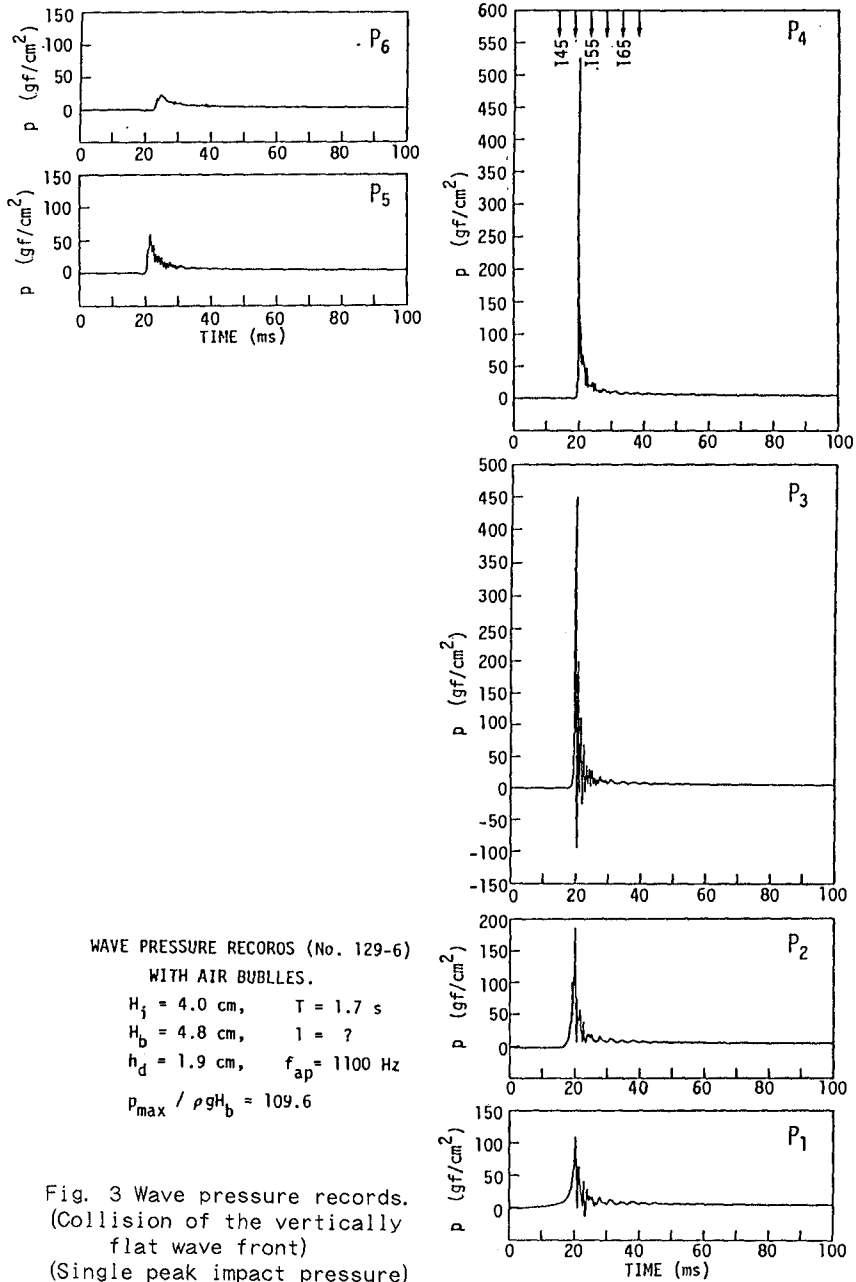bubbles to generation of the impact pressures.

Photo. 3 Sequence of the still pictures of the wave surface.
(Collision of the vertically flat wave front)

WAVE PRESSURE RECOROS (No. 129-6)
WITH AIR BUBLLES.

H_j = 4.0 cm,   T = 1.7 s
H_b = 4.8 cm, l = ?
h_d = 1.9 cm, f_{ap} = 1100 Hz

$p_{max} / \rho g H_b$ = 109.6

Fig. 3 Wave pressure records.
(Collision of the vertically
flat wave front)
(Single peak impact pressure)
(H_b=4. 8 cm, T=1. 7 s)

3.3 COLLISION OF PLUNGING BREAKERS -- DAMPED PRESSURE OSCILLATIONS
OF HIGH FREQUENCIES --

Photo. 4 gives the trapping process of a two dimensional air
pocket between the wall and wave. The pressure records at various
elevations in Fig. 4 show that the adiabatic action of the air
pocket gives rise not only to relatively high impact pressures on
the wall $(p_{max, 4}/ gH_b = 51.9)$, but also to damped oscillations with
a high frequencies of 250 Hz, immediately after a rapid pressure
drop. The pressure records in the air pocket zone (P_1-P_3) exhibit
almost the same variations both in magnitude and in phase. This
indicates repeated compression and expansion of the air pocket.
Immediately after the collision, the air pocket transforms into a
group of air bubbles, in which the bubbles rotate violently
(Photo. 4 (f)), and this will likely play some role in the reduc-
tion of pressure oscillations (Cooker and Peregrine, 1991). We can
not yet specify any dominant process of the energy dissipation due
to the violent motion of the air bubbles.
From the simultaneous records of the pressure and wave, we
found an evidence that damped pressure oscillations continue until
the air bubbles start to escape through the wave surface.

3.4 COLLISION OF FULLY DEVELOPED PLUNGING BREAKERS
-- DAMPED PRESSURE OSCILLATIONS OF LOW FREQUENCIES --

As plunging and curling of the breaking wave are developed, a
large cylindrical air pocket will be trapped and confined between
the wall and wave. As shown in Figs. 5 and 6, an increase of the
air pocket thickness 1, or the trapped air amount results in a
decrease both in the peak pressure p_{max} and in the frequency of
damped pressure oscillation, f_{ap}. Both p_{max} and f_{cap} are inversely
proportional to 1. However, the other principal characteristics of
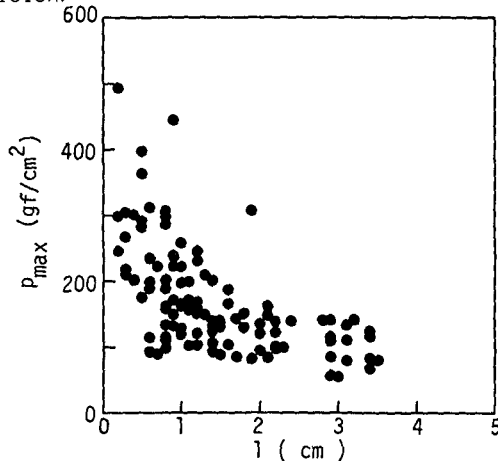the impact pressure are almost the same as those for the plunging
breaker collision.

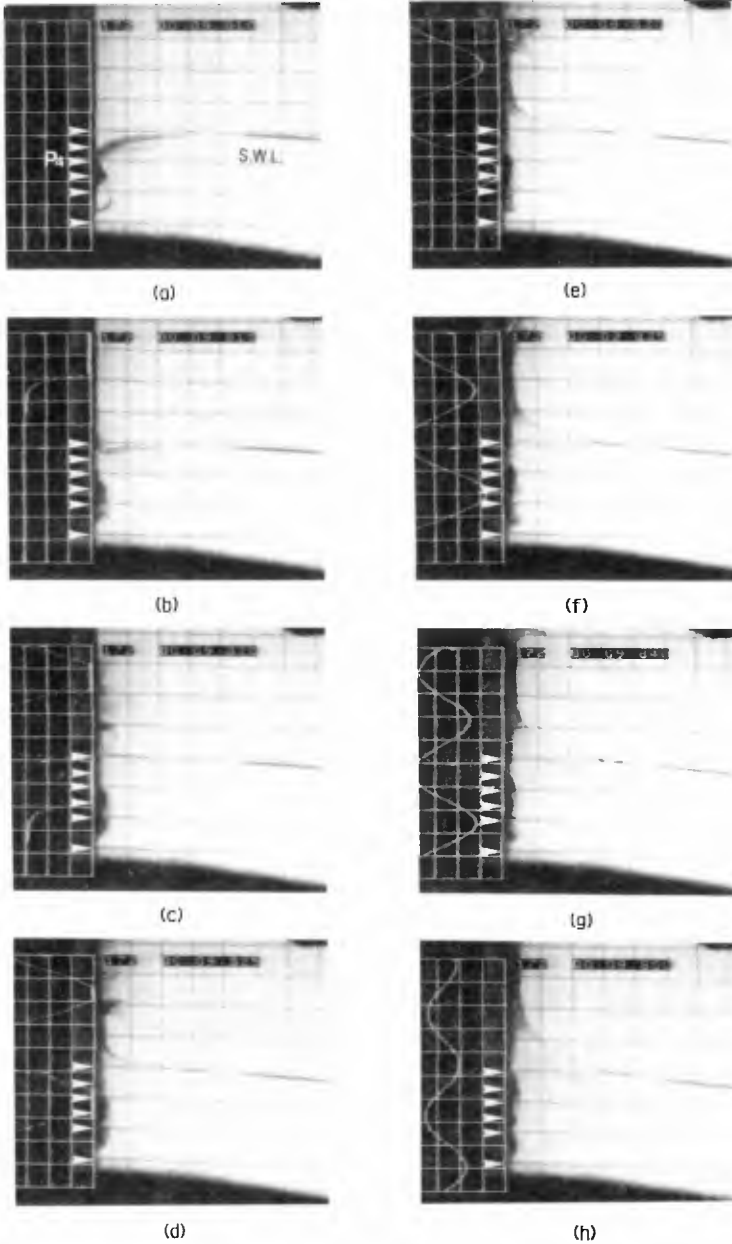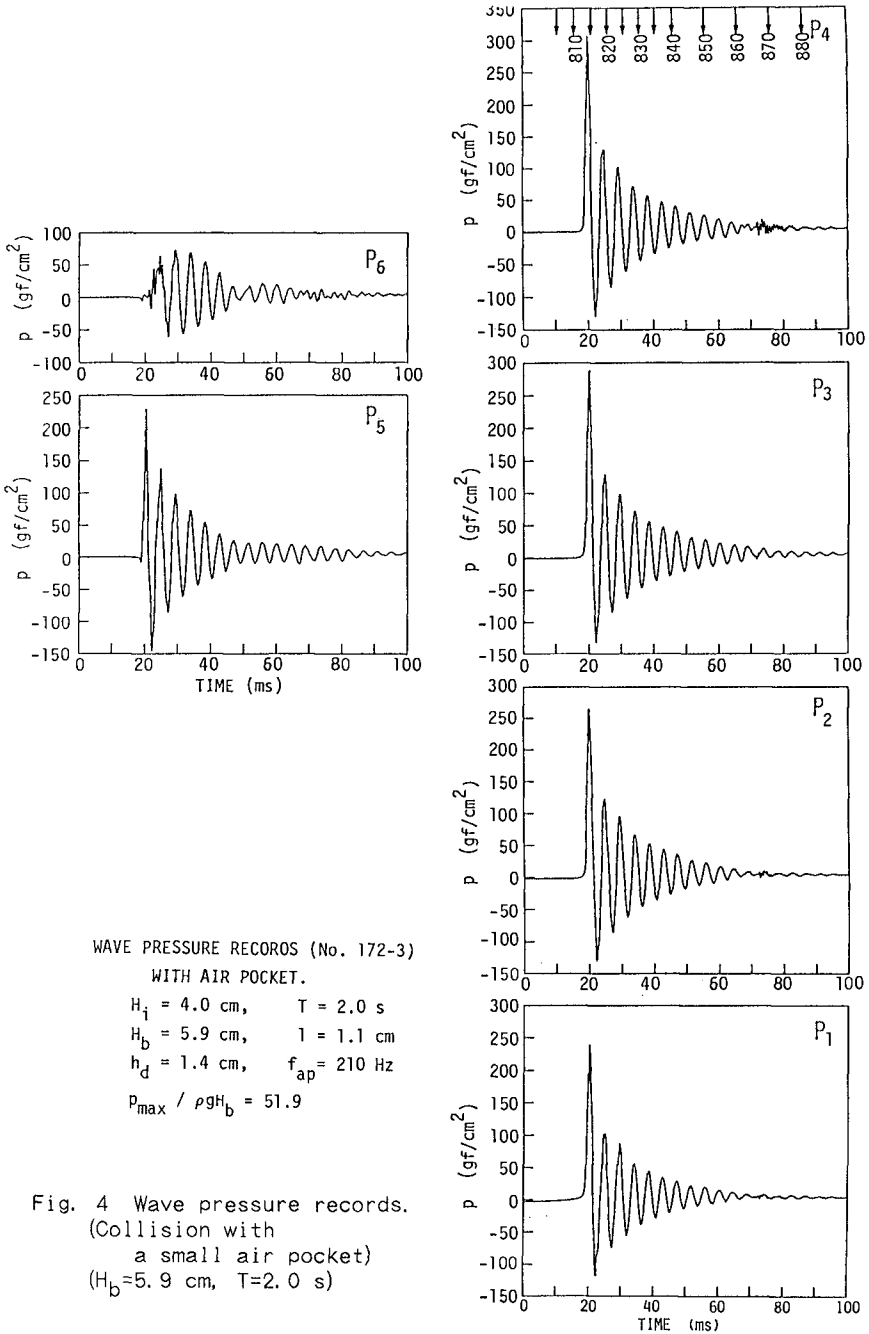Fig. 5 Relation between p_{max} and 1.

(a)

(b)

(c)

(d)

(e)

(f)

(g)

(h)

Photo. 4 Sequence of the still pictures of the wave surface.
(Collision with entrapping a small air pocket)

WAVE PRESSURE RECORDS (No. 172-3)
    WITH AIR POCKET.

H_i = 4.0 cm,   T = 2.0 s

H_b = 5.9 cm,   l = 1.1 cm

h_d = 1.4 cm, f_{ap}= 210 Hz

P_{max} / $\rho g H_b$ = 51.9

Fig. 4 Wave pressure records.
   (Collision with
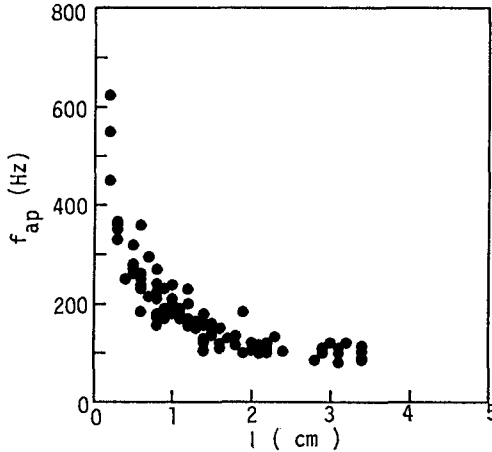   a small air pocket)
   (H_b=5.9 cm, T=2.0 s)

Fig. 6 Relation between f_{ap} and l.

6. PREDICTIVE MODEL

Predictive model for the impact pressure is developed under the following assumptions;

(1) The two dimensional air pocket can be substituted by a square pillar of width B, height d, and thickness l,

(2) The adiabatic process of the air pocket is represented by an equivalent spring system, as shown in Fig. 7, having apparent spring constant k, and

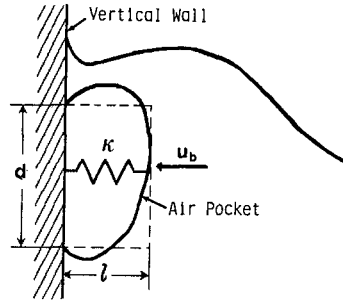(3) Radial oscillation and energy dissipation of the air pocket are ignored.

Fig. 7 Model of the air pocket.

The spring constant of the replaced air pocket can be written as $k = (Ed/l)E_v$, in which E_v $(=1.4\ p_{atm})$ is the bulk modulus of air and p_{atm} the atmospheric pressure. By introducing the virtual mass length K contributing the wave impact pressure (Bagnold, 1939), the maximum impact pressure p_{max} and the resonant frequency of the air pocket f_{ap} are obtained as

$$p_{max} = (\rho_w K E_v/l)^{1/2} u_b \qquad (1)$$

and

$$f_{ap} = (E_v/\rho_w Kl)^{1/2} \qquad (2)$$

, in which ρ_w is the density of the water, and u_b: forward velocity of the breaking wave front. The virtual mass length can be evaluated by measurements of impact pressure p, the rising time τ, and the forward velocity of wave front u_b (Bagnold, 1939):

$$K = \int_0^{\tau} p dt / \rho_w u_b \qquad (3)$$

Figs. 8 and 9 show the agreements between the model and measurement, $p_{max, M}/p_{max}$ and $f_{ap, M}/p_{ap}$, with respect to the air pocket thickness l, or the trapped air amount. Subscript M denotes the prediction. As seen in Fig. 8, due to the high variability in

measurement is not so good, especially when the air pocket is thin, $1 < 1$ cm. The agreement, however, becomes better with increasing the pocket thickness. From investigations of the measured data, we can specify the following main factors causing the high variability ; (1) The peak pressure region is much smaller than the diaphragm of pressure transducer, (2) The irregularity of the wave front changes the trapped air amount, and (3) The hitting location of wave crest tip is always shifted by high reflection of the wall. On the other hand, the model predicts reasonably well the frequency of the pressure oscillation, taking account of that the frequency should be lowered by boundary effects of the free surface, the bottom, and the wall (Topliss, Cooker, and Peregrine, 1992; Oumeraci and Partensckv, 1991).
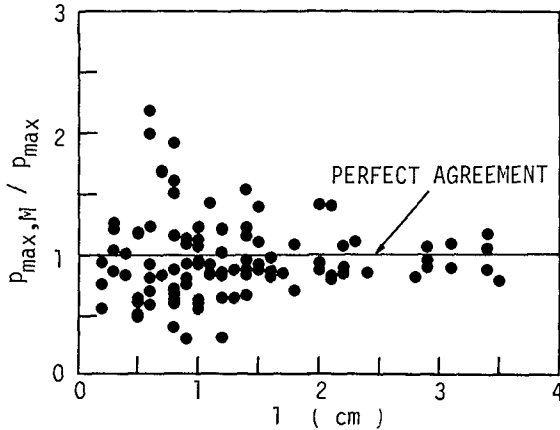
Fig. 8 Comparison between the predicted and measured
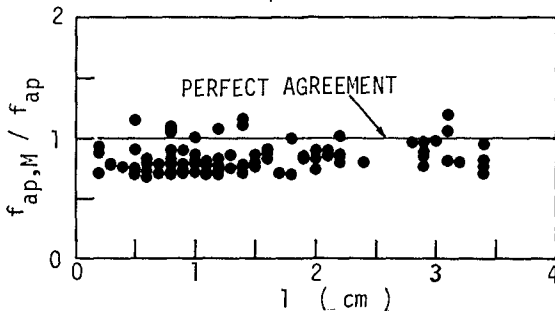maximum pressures.

Fig. 9 Comparison between the predicted and measured
frequencies of the damped pressure oscillation.

5. CONCLUDING REMARKS

     Simultaneous measurements of the impact pressure and the wave shape change clarify that air bubbles and air pocket entrapped between the wall and the wave plays a predominant role to the occurrence of the high impact pressure. The wave-impact process is

occurrence of the high impact pressure. The wave-impact process is characterized by the development of the wave breaking at impact, because of that the entrapped air amount depends critically on the impinging front shape of breaking waves onto the wall. The larger air amount trapped gives the lower impact peak pressure and the longer period of damped pressure oscillations immediately after the impact. The damped oscillation continues until the compressed air in the pocket starts to escape through the free surface.

The model proposed describes the wave-impact process and predicts the maximum pressure and the frequency of damped pressure oscillations, when the air pocket of two dimensional form is trapped between the wall and the wave. High variability in the wave-impact process deteriorates validity of the model.

REFERENCES

Arami, A. and M. Hattori (1988) : Experimental study on shock pressure of breaking waves, Proc. of Coastal Eng., JSCE, Vol. 36, pp. 579-583. (in Japanese)

Bagnold, R. A. (1939) : Interim report on wave pressure research, Jour. of ICE, Vol. 12, pp. 202-225.

Chen, E. S. and W. K. Melville (1988) : Deep-water plunging wave pressures on a vertical plane wall, Proc. of Royal Soc. London, A 417, pp. 95-131.

Cooker, M. J. and D. H. Peregrine (1991) : Wave breaking and wave impact pressures, Developments in Coastal Eng., Univ. of Bristol, pp. 47-64.

Mogridge, G. R. and W. W. Jamieson (1980) :Wave impact pressures, Proc. of 17th Conf. on Coastal Eng., pp. 1829-1848.

Oumeraci, H. and H. W. Partenscky (1991) : Effect of entrapped air on structure response, MAST G6-S Project 2, Proc. 1 st project workshop, Hannover.

Oumeraci, H. P. Klammer, and H. W. Partenscky (1991) : Classification of breaking wave impact loads on vertical structures, Submitted to ASCE, Jour. Waterways, Port, Coastal and Ocean Eng. Div.

Topliss, M., M. Cooker, and Peregrine (1992) : Pressure oscillations during wave impact on vertical walls, Proc. 23rd ICCE, Venice, ASCE.

Weggel, J. R. and W. H. Maxwell (1970) : Numerical model for wave pressure distributions, Proc. ASCE, Jour. of Waterways, Harbors and Coastal Eng. Div., No. WW3, pp. 623-641.